PAPER

Check for updates

Portable apparatus for high spatial and temporal resolution of *in situ* real-time surface albedo measurement in agricultural fields†

Sarah E. Eichler [ID] *

Climate models and global warming mitigation requires finer spatial data for albedo than satellites typically provide. To develop field-ready techniques for assessing albedo changes at the management unit scale, an affordable, highly portable albedometer is needed. This paper describes an apparatus to obtain real-time *in situ* measurements at sensor heights of 0.3 to 3 m providing direct albedo measurements for 8–1000 m^2 sensing area. This method allows sampling of multiple locations during a single near-solar-noon. The incoming and reflected solar radiation in an Ohio, USA cover-cropped agricultural field in winter showed a strong linear relationship that was not affected by time of day during 4 days of snowmelt. The portable apparatus is sufficiently sensitive to record changes in albedo resulting from hourly snowmelt. The influence of sensor height and thus footprint was analyzed by measuring albedo at a reduced tillage corn field and perennial forage field. Mean albedo ranged from 0.175 to 0.203. There were small but statistically significant differences between mean albedo within each site at different sensing footprints. These results suggest that heterogeneity in soil surface cover (vegetation and/or residue) within a single sensing footprint influences *in situ* surface albedo. It is important to examine similarly sized sensing footprints when comparing albedo across sites or monitoring a single site at multiple times especially in areas with heterogeneous surface cover. The method and equipment presented here will facilitate future research to better understood how albedo may be controlled through agricultural land management techniques for increased sustainability.

Environmental significance

Albedo is usually estimated for land areas >250 000 m^2 (25 ha) using 500 m resolution satellite pixels, yet it is recognized that heterogenous land surfaces are poorly represented by these data. A better understanding of real-time albedo at spatial and temporal scales of small agricultural fields could identify practices with enhanced albedo, and eventually verify climate smart agricultural systems. The portable albedometer demonstrated sensitivity to differences in albedo at sensing areas 8–1000 m^2. It could be used to monitor real-time albedo in small agricultural fields throughout the growing season and validate aerial albedo estimation methods.

1   Introduction

Globally there are over 47.9 million km^2 of agricultural land.[1] Over 3.6 million km^2 (900 million acres) of land are farmed in the United States alone.[2] This represents an enormous potential area in which to alter albedo for climate mitigation. However, it remains poorly understood whether beneficial albedo changes may be made using modest adjustments to agricultural production techniques for enhanced sustainability. Climate models and subsequent global warming mitigation requires finer spatial data and greater precision for albedo than satellites

can provide. Albedo estimates for modeling climate impacts from agriculture are commonly obtained from multispectral MODIS 500 m pixel resolution satellite measurements following processing of specific data bands (sensor wavelengths) and using narrow-to-broadband conversion computations, thus yielding albedo approximation for footprints ~250,000 m^2 at 16 day frequency[3–7] if cloud-free data are available. In combination with finer resolution data, MODIS albedo can be subsampled based on surface vegetation type, resulting in a synthetic albedo estimate for 900 m^2 for example using LANDSAT 30 m imagery.[8,9] Recent improvements to the resolution available from the satellite Sentinel-2 (10–20 m resolution) are being applied to the assessment of surface albedo on glaciers[10] and other landscapes.[11] These methods have been calibrated against near-surface (1 m) or tower based direct irradiance measurements. It is understood that the temporal and spatial scale of

Kent State University at Salem, Dept. Biological Sciences, 2491 St. Rt. 45 South, Salem, Ohio 44460, USA. E-mail: seeichle@kent.edu

† Electronic supplementary information (ESI) available: Time-lapse video of apparatus setup. See https://doi.org/10.1039/d1va00051a

© 2022 The Author(s). Published by the Royal Society of Chemistry

Environ. Sci.: Adv., 2022, **1**, 297–304 | **297**

albedo variation on Earth's surface is smaller than the 200–250 000 m^2 resolution of these satellite-based tools.[11–13] This is largely because vegetation and soil reflect incoming solar radiation differently throughout the year.[4,14–17] Comprehensive and consistent multispectral global data coverage remains the primary advantage of institutional satellites for calculating surface reflectance. However, even as higher resolution satellite systems become available, all satellite data must be adjusted for atmospheric interference, including clouds, aerosols, and particulates; and processed by geographic information system specialists. These cannot be used for real-time monitoring of albedo mitigation activities. Thus land and property managers are lacking a broadly-accessible method to measure albedo differences from surface management practices.

Efforts to manage surfaces and landscapes for desired albedo will need to be directed at much smaller spatial scales on the order of roof tops to farm fields or forest stands, that is, tens to thousands m^2. To obtain higher spatial and temporal resolution, broadband irradiance measurements that avoid interferences from clouds and atmospheric pollutants, towers have been used.[8,18] Towers holding sensors at 10–80 meters above the ground are permanent and expensive, yielding accurate, direct albedo data for >12000 m^2 sensing area on a near continuous basis. Fixed-wing aerial vehicle-mounted albedometers are temporary and expensive, but accurate and mobile, also providing high temporal resolution though for a limited time period. These have been used on snow-covered and glaciated settings, yielding transect data over kilometers by a few m wide from a single date.[10] MODIS and Landsat satellite albedo products do not effectively capture albedo changes during snow covered periods in heterogenous landscapes.[9] Thus, finer resolution albedo data from sensors <10 m above the surface may better describe variation in albedo during ephemeral snow cover on agricultural fields.

Neither the tower nor aerial approach is practical for monitoring changes in real-time albedo that may result from surface vegetation management on a seasonal basis. A method for obtaining high-resolution, *in situ* albedo has been described for a small UAV carrying a downward facing pyranometer 8–83 m above ground, but requires an expert, licensed pilot and integration using GIS while using a stationary upward-facing pyranometer on a tripod.[13] An earlier report of a ground-based portable field albedometer relied on silicon diodes with filters to offset known wavelength response problems[15] which provides insufficient precision for present earth system modeling research. Developments in the solar energy industry and a desire to monitor solar photovoltaic performance in real-time have led to broader access to affordable, fixed-location pyranometers used in making albedometers.

Others examined the usefulness of albedo estimates based on photographic red/blue/green band imagery from unmanned aerial vehicles[19,20] but there are known inaccuracies in converting these data to albedo estimates. These approaches provide larger potential coverage for landscape scale reflectance studies, but are not a solution for real-time monitoring.

Reports of *in situ* albedo over agricultural fields are less common and encompass a variety of methods. For example,

Jacobs and Van Pul[4] monitored albedo in non-irrigated forage maize during two growing seasons to compare modeling approaches. Zhang *et al.*[17] found diurnal and seasonal differences in albedo among several growth phases of spring wheat in 10 × 10 m research plots using pyranometers held 0.5 m above the canopy. A net radiometer was used to identify higher albedo in switchgrass compared to biofuel corn crops, however the sensing area is not stated.[21] Davin *et al.*[22] measured 0.1 higher albedo at 2 m above no-till compared to conventionally tilled wheat crops in a long-term research field in France, and cautioned that it is poorly understood how various soil and climate factors influence the observed difference.

To develop field-ready techniques for assessing albedo changes at the management unit scale such as farm fields, an affordable, highly portable albedometer is needed. This paper describes the configuration of an apparatus to obtain multiple albedo measurements at sensor heights of 0.3 to 3 m providing direct albedo measurements for 8–1000 m^2 sensing area. This method allows sampling of multiple locations during a single near-solar-noon; with setup, sampling, and sensor relocation accomplished by one researcher, using commercially available equipment. The portable apparatus was used to examine albedo during snowmelt, at different sensor heights, and within different agricultural crops in Ohio, USA.

2 Methods

2.1 Albedometer

Identical ISO 9060 spectrally flat Class B pyranometers were arranged in precisely opposite fields of view using a metal mounting plate fixed to a metal rod (albedometer kit, model SMP6V: Kipp & Zonen, OTT HydroMet USA; Table 1). These thermopile pyranometers have active temperature correction from −40 °C to +70 °C which easily encompasses the range of temperatures experienced at the study sites. The metal rod was attached at level to the boom (Fig. 1). Cables from each pyranometer were secured in tandem using plastic zip ties. These sensor cables were secured temporarily to the boom by hooking them over the jib adjustment knobs and down to the data logger on the tripod. The albedometer, rod, and cables are removed as one unit and stored in protective foam for transport.

Sensor height can be adjusted primarily *via* the universal contractor's elevating aluminum tripod with extendible legs and adjustable neck (**https://Tigersupplies.com**, Table 1). The tripod was modified by the addition of a threaded swivel spud socket with lockable screw (Fig. 1A) at the top of the neck to receive a portable, telescoping, self-leveling camera jib (model JB4, **https://GlideGear.net**) with addition of customized swivel spud (B), creating a sensor boom. A machined thread and hand tightening bolt (D) was added to the sensor end of the jib which attached to a rod clamp (C).

Counterweight was added to the jib with attached albedometer. An adjustable strap secured the jib at desired angle by bracing the jib to the tripod. The height of the albedometer was adjusted first through the tripod legs and neck, and finally by the jib angle, with preference for a jib angle nearer horizontal. Windy conditions may require height adjustment below the

Table 1 Physical characteristics and source for portable albedometer components

	Largest dimension[a] (cm)	Weight (kg)	Cost (US$)	Source
Tripod	122–225	14.8	109	Tiger Supplies
Jib	55–135	5.2	120	Glide Gear
Counterweight	12	5.6	5	Resale store
Carrying bag	86	5.4	5	Resale store
Meteon data logger	17	0.6	<1000	OTT HydroMet
Kipp Zonen SMP6V albedometer	15	5.6[b]	<4000	OTT HydroMet
Total		37.2	<5240	

[a] Multiple values indicate contracted (for transporting) and expanded to maximum functioning dimensions. [b] Includes 10 m cabling for each pyranometer, attached metal plate, and rod.
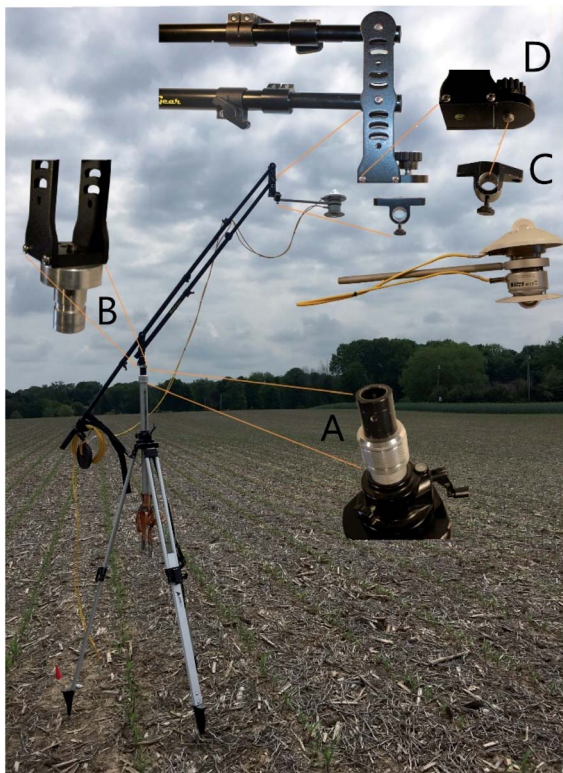

Fig. 1 Portable apparatus for measuring *in situ* albedo at Site 1. The height of the albedometer is raised or lowered through a combination of tripod leg adjustments and changing the angle of the sensor boom. A threaded spud socket (A) on the tripod and swivel spud (B) allows adjustment of the sensor boom. A rod clamp (C) is attached to sensor boom with machined, hand-tightening bolt (D).

hypothetical maximum. To avoid shade and reflectance interference from the apparatus, it is arranged for use in the Northern Hemisphere so that the albedometer is due South of the tripod and the jib is aligned on a North/South direction.

The albedometer, jib, and small sensor accessories were fitted into the compartments of a used golf bag with padded backpack straps and kickstand. The albedometer rod was inserted into a foam pool noodle trimmed to fit inside one of the bag compartments to secure it for transportation. The tripod was carried separately. A time-lapse video of the setup is available in the ESI.†

According to the pyranometer manufacturer, 99% of the signal will originate from the circular area using a radius of sensor height multiplied by ten.[23] We apply the formula from ref. 13 in which the sensing area arises from a circle with a diameter ("footprint") that is twice the sensor height multiplied by the tan of the sensor half field of view (eqn (1)). The effective half field of view for this pyranometer is 81 degrees.

$$\text{Footprint diameter} = 2 \times \text{height} \times \tan(\text{effective half field of view}) \quad (1)$$

Sensor height is measured in the field as the distance between the soil and the metal rod, minus 6 cm to account for the distance between peak of the dome and rod. The apparatus used for this study can be set at heights from 0.3–3 m (Table 2).

A Meteon 2.0 data logger (OTT HydroMet, USA) was programmed to log at 1 or 15 s intervals after a manual start-log command. The minimum, maximum, and average radiation (W m^{-2}) is recorded for each interval, on each pyranometer: sensor 1 is sky-facing, sensor 2 is ground facing. After retrieving logged data, albedo was calculated for each interval as: sensor 2 W m^{-2}/sensor 1 W m^{-2}. The mean albedo for any given monitoring period (10 minutes minimum) is calculated as the average of the interval albedo values, excluding the first and last minute of the monitored period, to avoid readings when the researcher is within the sensing area.

2.2 Study sites

Data were collected from rainfed agricultural fields in Portage County, Ohio, USA. The area is characterized by flat to gently rolling topography, patchy landscapes including forest, annual crops, perennial forage crops, and residential areas (Fig. 2).

Table 2 Albedo sensing footprint relative to portable albedometer height above soil surface

Sensor height (m)	Sensing diameter (footprint) (m)	Sensing area (m²)
0.3	3.0	7
0.6	6.8	36
0.9	10.6	88
1.5	18.2	260
2.0	24.5	471
3.0	37.0	1082

© 2022 The Author(s). Published by the Royal Society of Chemistry

Environ. Sci.: Adv., 2022, **1**, 297–304 | **299**

Fig. 2 Aerial photograph showing mixed agricultural, forested, and residential patches surrounding study sites 1 and 2; Portage County, Ohio USA.

Individual management units (fields) are typically less than 20 hectares. Site 1 is located in a reduced-tillage, annually cropped field consisting of Chili loam soils 2 to 6 percent slopes.[24] Site 1 contained grain corn (*Zea mays*) drilled May 2021, cereal rye (*Secale cereale*) cover crop in Winter 2021 and Fall 2020 (herbicide terminated), following harvest of grain soybean (*Glycine max*) in late summer 2020. Prior to broadcast cover crop planting, soybean residue was distributed by a Salford RTS vertical tillage implement. This site contained cereal rye cover crop in fall 2019 and grain corn during summer 2019. Both corn stalks and soybean stem residues were visible on the soil surface during 2021 data collection. Site 2 is located approximately 200 m north of Site 1 in an untilled, regularly harvested, hay field consisting of Jimtown loam soils 2 to 6 percent slopes.[24] Both sites were unshaded by other vegetation or structures during data collection timeframe of 10:00 to 16:00 Eastern Time zone.

Environmental data including air temperature, wind speed, and humidity were recorded using a mini-environmental quality meter after acclimating for two minutes (model 850070; Sper Scientific, Ltd). Green vegetation was quantified as percent cover using the Canopeo app for iPhone.[25]

2.3 Monitoring albedo during snowmelt

The albedometer was positioned 2.0 m above the soil at Site 1 between 10:00–16:00 Eastern Time on four consecutive dates following a significant snow precipitation event. Environmental data were collected at the start and end of the albedo monitoring period. Pyranometer data were logged in 15 s intervals.

2.4 Detecting albedo at different sensor footprints

On three dates during the spring and summer growing season (24 May, 24 June, and 27 July 2021), albedo was measured at

Table 3 Environmental and site conditions

Date	Site	Air temp. (°C)	Wind max (m s^{-1})	Wind min (m s^{-1})	Relative humidity (%)	Green vegetation cover (%)	Vegetation height (cm)	Beginning incoming radiation (W m^{-2})
2/23/2021	1	6.8	2.9	1.2	59	0.00	a	269
2/24/2021	1	7.3	5.4	1.4	53	0.00	a	486
2/25/2021	1	5.9	2.2	0	46	0.01	3	516
2/26/2021	1	2.1	2.1	0.5	60.4	0.01	3	286
5/24/2021	1	28.2	1.4	0	53	1.41	23	809
6/24/2021	1	23.5	1.6	0.4	58.6	71.80	145	758
7/27/2021	1						275	922
7/27/2021	2	34.2	3.8	0.5	51.5	71.78	28	848

a Vegetation was snow covered; measured on subsequent dates when snow had melted from patches.

© 2022 The Author(s). Published by the Royal Society of Chemistry

multiple sensor heights, and thus footprints, at Site 1. On 27 July a comparison was made at Site 2. Sensor height was adjusted by raising or lowering the jib and extendable neck of the tripod, without moving the tripod legs. Each albedo measurement occurred over 10 minutes.

Descriptive and comparative statistics were completed using JMP 16.0.0 software (SAS Institute Inc. 2021).

3 Results and discussion

3.1 Monitoring *in situ* real-time albedo during snowmelt

Environmental conditions for each observation date are listed in Table 3. At the dates of snowmelt monitoring, Site 1 was cover-cropped with winter rye though very little green vegetation cover was present (0.01%). Precipitation left approximately 12 cm snow at Site 1 prior to measurements on Feb 22, 2021. On Feb 23, the snow had compacted slightly to approximately 7 cm. The entire field appeared fully covered by snow. By Feb 26, snow was patchy; with soil, crop residue, and/or cover crop visible on about half the field. Summary statistics for real-time albedo observed during four days of snowmelt are provided in Table 4.

A gradual decrease in albedo was observed during snowmelt at Site 1, from a maximum of 0.75 on February 23, to a minimum of 0.18 on Feb 26 (Fig. 3). The Site 1 data falls between net radiometer albedo values reported for agricultural research plots receiving tillage and/or manure treatments.[26] They found albedo dropped from 0.89 to 0.46 over 2 days following snowfall on an un-manured, no-tillage plot whereas

Table 4 Summary statistics for surface albedo during snowmelt on reduced tillage, cover-cropped agricultural field. *N* indicates the number of 15 s interval calculations of reflected: incoming radiation

	N	Min	Max	Average	CV
2/23/2021	682	0.61	0.75	0.68	6.22
2/24/2021	1369	0.56	0.65	0.60	3.03
2/25/2021	441	0.25	0.39	0.34	8.89
2/26/2021	1440	0.18	0.29	0.23	12.17
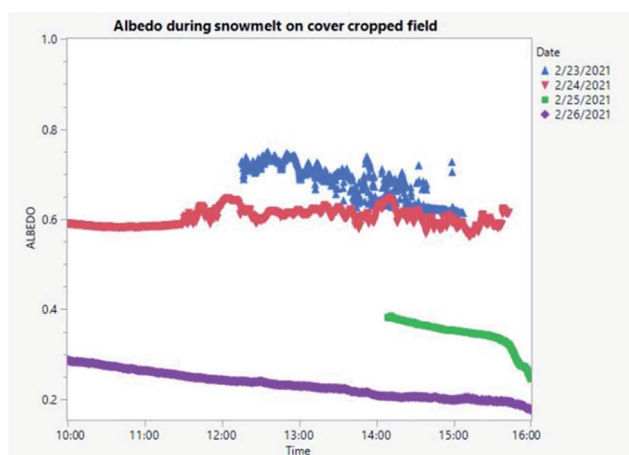
Fig. 3 Albedo during four days of snowmelt in an agricultural field.
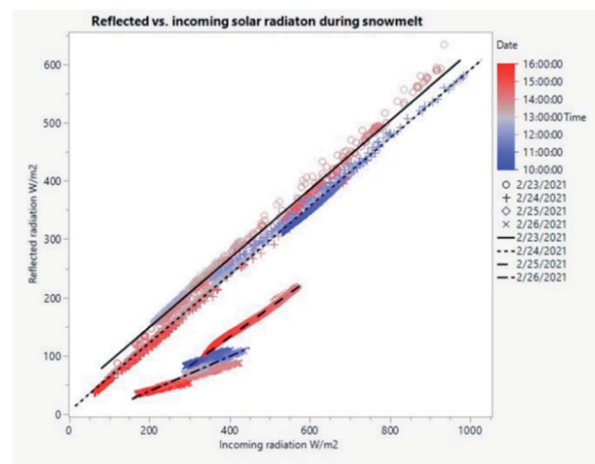
Fig. 4 Relationship between incoming and reflected radiation changes during snowmelt in an agricultural field.

manured areas had a minimum albedo of 0.12. Due to the challenges of capturing fine temporal resolution on multiple plots, later snow melt information and albedo changes were estimated using a multiple linear regression model in that study.[26]

The incoming and reflected solar radiation showed a strong linear relationship that was not affected by time of day (Fig. 4). This relationship indicates these pyranometers are independently sensitive to changes in actual radiation despite the continuously changing angle of sunlight. The slope of linear regressions decreased each day as snowmelt progressed, from 0.59 on day one Feb 23 to 0.30 on Feb 26 (Table 5). The relationship was weakest on the fourth day when snow cover was patchy ($R^2 = 0.88$ compared to 0.99 on Feb 23). In the present study, an alternative method of calculating average daily albedo from the slope as in ref. 4 narrows the difference between the dates, underestimating albedo during full snow cover and overestimating albedo when snow is patchy. The portable apparatus is sufficiently sensitive to record changes in albedo resulting from incremental snow melt despite potential error contributed by shifting angle of incoming radiation. Such error may be minimized by using the interval albedo rather than a daily average based on slope of reflected *versus* incoming radiation.

Satellite databases were examined for albedo data corresponding to the snow melt observations. An albedo product is sometimes available for MODIS data but no satellite passes

Table 5 Linear relationship between incoming (*X*) and reflected (*Y*) radiation measured by opposite-facing pyranometers during snowmelt on reduced-tillage, cover-cropped field

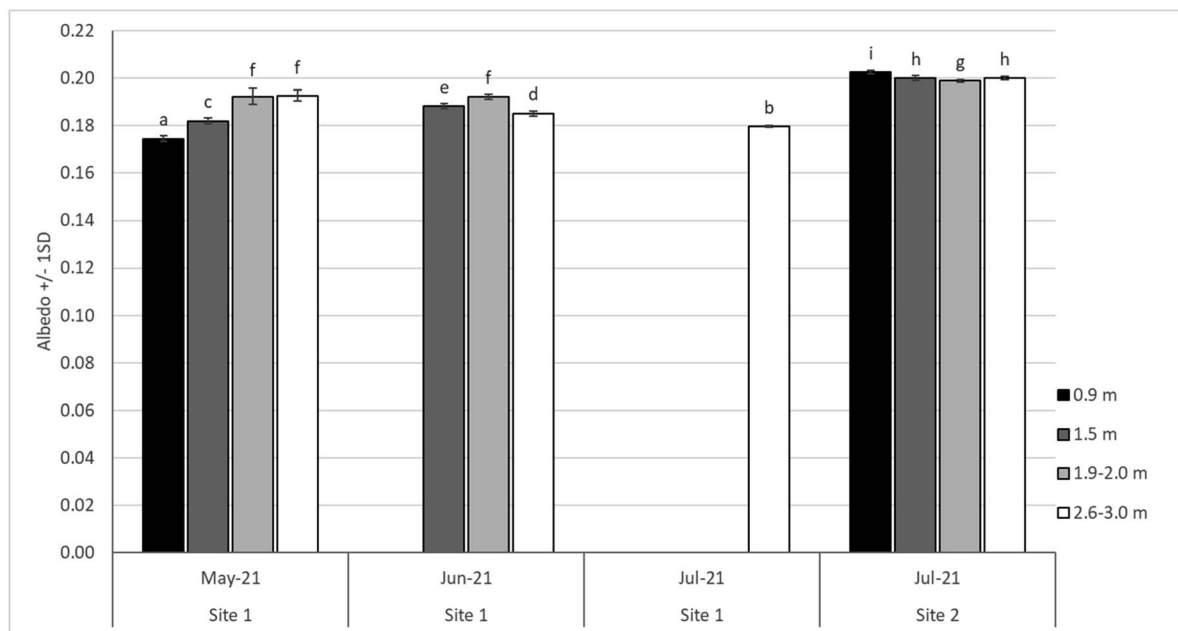| Date	RMSE	R^2	*P*	*F*	Intercept	Slope
2/23/2021	9.5	0.99	<0.0001	91 531	31.01	0.5905
2/24/2021	6.46	1.00	<0.0001	45 176	5.333	0.5854
2/25/2021	3.44	0.99	<0.0001	50 064	−67.86	0.501
2/26/2021	7.39	0.88	<0.0001	10 585	−20.81	0.2997

Fig. 5 Mean albedo measured at different sensor heights and growing season dates in corn (Site 1) and hay (Site 2) crops. Letters indicate statistical difference at alpha = 0.05 using repeated measures factorial ANOVA followed by Tukey HSD. At Site 1, data was excluded for low (June) and low, medium, and high (July) sensor heights because corn height exceeded sensor height.

occurred within a reasonable time frame of this experiment. Sentinel satellite host sites do not provide an albedo product but instead have a snow cover imagery product which was available for Feb 20, 2021 for comparison to surface data. Both true-color and snow cover images indicate complete, uninterrupted snow cover which lacks the detail available from surface observations with the portable albedometer at Site 1 during the experiment (ESI figures).†

3.2 *In situ* real-time albedo differs according to sensing footprint

To analyze the influence of sensor height and thus sensing footprint, real-time albedo was measured on three dates during the growing season using multiple sensor height settings from 0.9 to 3 m above the soil, representing sensing areas of 88–1082 m². Measurements obtained from below the crop canopy were excluded (Site 1: June low; July low, medium, high) due to the large variability in albedo resulting from sensor 1 being irregularly shaded by the movement of corn leaves in the breeze.

When albedo data are pooled across sites and dates, there is no effect of sensor footprint ($p = 0.63$). A repeated measures factorial ANOVA was completed using site + date as the subject, and sensor height as the within-subject factor after categorizing as low, medium, high, or very high (corresponding to 0.9, 1.5, 1.9–2.0, and 2.6–3.0 m above soil), followed by Tukey HSD. Mean albedo during the growing season ranged from 0.175 to 0.203 with comparable standard error among categories (0.00014–0.00026). There were small but statistically significant differences between mean albedo within each site at different sensor heights (Fig. 5). Site 2 (hayfield) had higher albedo at each sensor footprint compared to Site 1 (corn). Despite the

simple approach to calculating albedo presented here, which does not include distinctions between direct and diffuse irradiation,[4] crop phenology,[16,17] or solar angle,[16] the portable apparatus for determining real-time *in situ* albedo is sensitive to differences among crops, seasons, and sensor footprints. These results indicate that crop and/or surface residue factors drive differences in albedo at areas <1000 m². These results suggest that heterogeneity in soil surface cover (vegetation, residue, soil) within a single sensing area influences *in situ* real-time surface albedo measurements. It is important to examine similarly sized sensing footprints when comparing albedo across sites or monitoring a single site at multiple times.

4 Conclusions

The incoming and reflected solar radiation in an Ohio, USA cover-cropped agricultural field in winter showed a strong linear relationship that was not affected by time of day during 4 days of snowmelt. The influence of sensor height and thus footprint was analyzed by measuring real-time albedo at a reduced tillage corn field and perennial forage field during the growing season. There were small but statistically significant differences between mean albedo within each site at different sensing footprints. The straightforward procedure used in the study could be employed by resource managers to monitor changes in albedo, for example, in order to identify progress toward climate smart agricultural practices or to verify mitigation activities. The apparatus described here is sufficiently sensitive to study farm management changes that could enhance albedo.

Additional research is needed to identify crop, residue, and soil characteristics or interactions that influence real-time

albedo within the small footprints reported in this study. The method and equipment presented here will facilitate such research.

Additional data are needed to identify whether factors such as crop height, cultivar, wind speed, or residue influence *in situ* real-time albedo at field scale during winter and throughout crop growth. The ability to rapidly deploy a portable apparatus, such as the one described here, will facilitate calibration of aerial estimates or satellite-based models of albedo at high spatial and temporal resolution.

Improved understanding of land management factors controlling albedo as well as interactions between albedo and local climate (cooling, humidity, soil moisture, *etc.*) are needed to develop recommendations for adaptive management.

Author contributions

S. Eichler conceived of the project, collected all field measurements, analysed data, and completed the first and subsequent written drafts.

Conflicts of interest

There are no conflicts to declare.

Acknowledgements

References

1 United Nations Food and Agriculture Organization, *Agricultural Land (square kilometers)*, FAOSTAT, 2018, available from: **https://data.worldbank.org/indicator/ AG.LND.AGRI.K2.**

2 USDA, National Agricultural Statistics Service, *2017 Census of Agriculture United States Summary and State Data*, 2019.

3 C. Schaaf and Z. Wang, *MCD43A1 MODIS/Terra + Aqua BRDF/ Albedo Model Parameters Daily L3 Global – 500 m V006. NASA EOSDIS Land Processes DAAC*, 2015.

4 A. F. G. Jacobs and W. A. J. van Pul, Seasonal changes in the albedo of a maize crop during two seasons, *Agric. For. Meteorol.*, 1990, **49**(4), 351–360.

5 C. A. Barnes and D. P. Roy, Radiative forcing over the conterminous United States due to contemporary land cover land use albedo change, *Geophys. Res. Lett.*, 2008, **35**(L09706), 1–6.

6 Z. Münch, L. Gibson and A. Palmer, Monitoring Effects of Land Cover Change on Biophysical Drivers in Rangelands Using Albedo, *Land*, 2019, **8**(2), 33.

7 P. Sciusco, J. Chen, M. Abraha, C. Lei, G. P. Robertson, R. Lafortezza, *et al.*, Spatiotemporal variations of albedo in managed agricultural landscapes: inferences to global warming impacts (GWI), *Landsc. Ecol.*, 2020, **35**(35), 1385–1402.

8 Z. Wang, C. B. Schaaf, Q. Sun, J. H. Kim, A. M. Erb, F. Gao, *et al.*, Monitoring land surface albedo and vegetation dynamics using high spatial and temporal resolution synthetic time series from Landsat and the MODIS BRDF/ NBAR/albedo product, *Int. J. Appl. Earth Obs. Geoinf.*, 2017, **59**, 104–117.

9 Z. Wang, C. B. Schaaf, A. H. Strahler, M. J. Chopping, M. O. Román, Y. Shuai, *et al.*, Evaluation of MODIS albedo product (MCD43A) over grassland, agriculture and forest surface types during dormant and snow-covered periods, *Remote Sens. Environ.*, 2014, **140**, 60–77.

10 K. Naegeli, A. Damm, M. Huss, H. Wulf, M. Schaepman and M. Hoelzle, Cross-comparison of albedo products for glacier surfaces derived from airborne and satellite (Sentinel-2 and Landsat 8) optical data, *Remote Sens. Environ.*, 2017, **9**(2), 110.

11 Z. Li, A. Erb, Q. Sun, Y. Liu, Y. Shuai, Z. Wang, *et al.*, Preliminary assessment of 20-m surface albedo retrievals from sentinel-2A surface reflectance and MODIS/VIIRS surface anisotropy measures, *Remote Sens. Environ.*, 2018, **217**, 352–365.

12 C. H. Reijmer, W. H. Knap and J. Oerlemans, *The surface albedo of the vatnajökull ice cap, iceland: a comparison between satellite-derived and ground-based measurements*, 1999.

13 C. R. Levy, E. Burakowski and A. D. Richardson, Novel measurements of fine-scale albedo: using a commercial quadcopter to measure radiation fluxes, *Remote Sens. Environ.*, 2018, **10**(8), 1303.

14 M. Georgescu, D. B. Lobell and C. B. Field, Direct climate effects of perennial bioenergy crops in the United States, *Proc. Natl. Acad. Sci. U. S. A.*, 2011, **108**(11), 4307–4312.

15 J. C. H. van der Hage, Interpretation of Field Measurements Made with a Portable Albedometer, *J. Atmos. Ocean. Technol.*, 1992, **9**, 420–425.

16 J. Song, Phenological Influences on the albedoof prairie grassland and crop fields, *Int. J. Biometeorol.*, 1999, **42**, 153–157.

17 Y. F. Zhang, X. P. Wang, Y.-X. Pan and R. Hu, Diurnal and seasonal variations of surface albedo in a spring wheat field of arid lands of Northwestern China, *Int. J. Biometeorol.*, 2013, **57**, 67–73.

18 J. J. Michalsky and G. B. Hodges, Field measured spectral albedo-four years of data from the western u.s. Prairie, *J. Geophys. Res.: Atmos.*, 2013, **118**(2), 813–825.

© 2022 The Author(s). Published by the Royal Society of Chemistry

Environ. Sci.: Adv., 2022, **1**, 297–304 | **303**

19 C. Cao, X. Lee, J. Muhlhausen, L. Bonneau and J. Xu, Measuring landscape albedo using unmanned aerial vehicles, *Remote Sens. Environ.*, 2018, **10**(11), 1812.

20 J. C. Ryan, A. Hubbard, J. E. Box, S. Brough, K. Cameron, J. M. Cook, *et al.*, Derivation of High Spatial Resolution Albedo from UAV Digital Imagery: Application over the Greenland Ice Sheet, *Front. Earth Sci.*, 2017, **5**, 40.

21 E. Eichelmann, C. Wagner-Riddle, J. Warland, B. Deen and P. Voroney, Comparison of carbon budget, evapotranspiration, and albedo effect between the biofuel crops switchgrass and corn, *Agric., Ecosyst. Environ.*, 2016, **231**, 271–282.

22 E. L. Davin, S. I. Seneviratne, P. Ciais, A. Olioso and T. Wang, Preferential cooling of hot extremes from cropland albedo management, *Proc. Natl. Acad. Sci. U. S. A.*, 2014, **111**(27), 9757–9761.

23 Kipp & Zonen, *Instruction Manual, CMP series Pyranometer and CMA series Albedometer Publication V1610*, Delft, 2016, available from: **https://www.kippzonen.com/Download/72/Manual-Pyranometers-CMP-series-English?ShowInfo=true**.

24 Soil Survey Staff, *Natural Resources Conservation Service, USDA*, Web Soil Survey, 2021, available from: **https://websoilsurvey.sc.egov.usda.gov/**.

25 A. Patrignani and T. E. Ochsner, Canopeo: a powerful new tool for measuring fractional green canopy cover, *Agron. J.*, 2015, **107**(6), 2312–2320.

26 M. N. Stock, F. J. Arriaga, P. A. Vadas and K. G. Karthikeyan, Manure application timing drives energy absorption for snowmelt on an agricultural soil, *J. Hydrol.*, 2019, **569**, 51–60.